Synthesis, Characterization, Cytotoxic Activity, and Metabolic Studies of Ruthenium(II) Polypyridyl Complexes Containing Flavonoid Ligands

Alexandra-Cristina Munteanu, Anna Notaro, Marta Jakubaszek, Joseph Cowell, Mickaël Tharaud, Bruno Goud, Valentina Uivarosi, Gilles Gasser

Synthesis, Characterisation, Cytotoxic Activity and Metabolic Studies of Ruthenium(II) Polypyridyl Complexes containing Flavonoid Ligands

Alexandra-Cristina Munteanu,[a,#] Anna Notaro,[b,#] Marta Jakubaszek,[b,c] Joseph Cowell,[b] Mickaël Tharaud,[d] Bruno Goud,[c] Valentina Uivarosi,[a] and Gilles Gasser[b,]*

[a] Department of General and Inorganic Chemistry, Faculty of Pharmacy, "Carol Davila" University of Medicine and Pharmacy, 020956 Bucharest, Romania.

[b] Chimie ParisTech, PSL University, CNRS, Institute of Chemistry for Life and Health Sciences, Laboratory for Inorganic Chemical Biology, F-75005 Paris, France.

[c] Institut Curie, PSL University, CNRS UMR 144, Paris, France.

[d] Université de Paris, Institut de Physique du Globe de Paris, CNRS, F-75005 Paris, France.

[#] these authors have contributed equally to the work

* Corresponding author: E-mail: gilles.gasser@chimeparistech.psl.eu; WWW: www.gassergroup.com; Phone: +33 1 44 27 56 02

ORCID Number

Alexandra-Cristina Munteanu: 0000-0003-4704-5401

Anna Notaro: 0000-0003-0148-1160

Marta Jakubaszek: 0000-0001-7590-2330

Joseph Cowell: 0000-0001-8750-7223

Bruno Goud: 0000-0003-1227-4159

Valentina Uivarosi: 0000-0002-7165-5069

Gilles Gasser: 0000-0002-4244-5097

Keywords: Bioinorganic Chemistry, Cancer, Flavonoid, Medicinal Inorganic Chemistry, Ruthenium.

Abstract

Four novel monocationic Ru(II) polypyridyl complexes have been synthesized with the general formula $[Ru(DIP)_2flv]X$, where DIP is 4,7-diphenyl-1,10-phenanthroline, flv stands for the flavonoid ligand (5-hydroxyflavone in **$[Ru(DIP)_2(5\text{-}OHF)](PF_6)$**, genistein in **$[Ru(DIP)_2(gen)](PF_6)$**, chrysin in **$[Ru(DIP)_2(chr)](OTf)$**, and morin in **$[Ru(DIP)_2(mor)](OTf)$**) and X is the counterion, PF_6^-, and OTf^- (triflate, $CF_3SO_3^-$), respectively. Following the chemical characterisation of the complexes by ^1H and ^{13}C-NMR, mass spectrometry and elemental analysis, their cytotoxicity was tested against several cancer cell lines. The most promising complex, **$[Ru(DIP)_2(gen)](PF_6)$**, was further investigated for its biological activity. Metabolic studies revealed that this complex severely impaired mitochondrial respiration and glycolysis processes, contrary to its precursor, **$Ru(DIP)_2Cl_2$**, which showed a prominent effect only on the mitochondrial respiration. In addition, its preferential accumulation in MDA-MB-435S cells (a human melanoma cell line previously described as mammary gland/breast; derived from metastatic site: pleural effusion), that are used for the study of metastasis, explained the better activity in this cell line compared to MCF-7 (human, ductal carcinoma).

Introduction

Cancer, listed as a chronic degenerative non-communicable disease by the World Health Organization (WHO), is a leading cause of death worldwide.[1] Despite the clinical success of several platinum-based drugs (e.g., cisplatin, carboplatin and oxaliplatin),[2] their efficacy is impeded by intrinsic and acquired resistance, and dose-limiting toxicity.[3] Therefore, the search for more effective therapeutic strategies has led to the development of other metal complexes with anticancer properties.[4] Ruthenium (Ru)-based compounds have emerged as potential anticancer drug candidates due to their unique physico-chemical and biological properties, [5–8] generally lower systemic toxicity (in animal models) and higher cellular uptake compared to platinum complexes.[5] NAMI-A, [9,10] KP1019 [11,12] and its water-soluble sodium salt IT-139 (formerly KP1339)[13] are Ru complexes that have been evaluated in clinical trials as chemotherapeutic agents for the treatment of cancer. NAMI-A is an antimetastatic drug candidate with diverse mechanisms of action.[14–17] Unfortunately, during a phase I/II study, its clinical activity was found to be disappointing, which led to the discontinuation of the trials. These poor results were mainly attributed to dose-limiting adverse events associated with the treatments.[10]

Therefore, current trends in the development of novel Ru-based anticancer drug candidates aim to meet the need for more efficient treatments and improved toxicological profiles for the emergent drugs. For instance, Ru(II) polypyridyl complexes have shown great potential,[18,19] finding applications in tumour diagnosis,[20] as antineoplastic agents[19,21] or photosensitizers for PDT.[22,23] The most successful compound bearing a Ru(II) polypyridyl scaffold, TLD-1433,[24] has recently entered phase II clinical studies as a photosensitizer for intravesical photodynamic therapy (PDT) against bladder cancer.[25,26]

Moreover, very interesting results have been found for heteroleptic complexes of Ru(II), bearing an *O,O*-chelating ligand. For instance, RAPTA complexes with curcuminoid ligands (IC_{50} values ≤ 1 μM) displayed novel binding modes with biomolecular targets and high, cancer cell selective activity.[27] In addition, $Ru^{II}(\eta^6$-*p*-cymene) complexes with flavonol-derived ligands were found to have potent cytotoxic activity against several human cancer cell lines, with IC_{50} values in the low micromolar range.[28]

These recent discoveries have prompted us towards the study of the therapeutic potential of Ru(II) polypyridyl complexes with the flavonoids shown in Figure 1, as *O,O*-chelating ligands. Flavonoids are a naturally occurring subclass of polyphenols, with high structural versatility.[29] They have been extensively studied in the design of novel anticancer drug candidates. As a result, two derivatives of the flavonoid chrysin (Figure 1), namely flavopiridol and P276-00, have entered clinical trials.[30,31] Although not yet fully understood, the cytotoxic activity of flavonoids is believed to rely upon the modulation of cellular processes that include proliferation, differentiation, apoptosis, metastasis and oxidative stress.[29,32,33] Moreover, naturally occurring flavonoid aglycons display exceptionally low, if any, systemic toxicity. It should be noted, however, that the absence of acute toxic effects is related to their low water solubility and bioavailability. [34,35]

The present work focuses on the synthesis of four novel monocationic Ru(II)-polypyridyl complexes with the general formula $[Ru(DIP)_2flv]X$, where DIP is 4,7-diphenyl-1,10-phenanthroline, flv stands for the flavonoid ligand (5-hydroxyflavone in **$[Ru(DIP)_2(5\text{-}OHF)](PF_6)$**, genistein in **$[Ru(DIP)_2(gen)](PF_6)$**, chrysin in **$[Ru(DIP)_2(chr)](OTf)$**, and morin in **$[Ru(DIP)_2(mor)](OTf)$**) and X is the counterion (PF_6^- or OTf^- (triflate)). Following the successful synthesis and characterisation, the antiproliferative activity of the complexes was tested against

different cell lines. For the most potent compound of the series, metabolic studies were performed and compared with the **$Ru(DIP)_2Cl_2$** precursor.

Results and Discussion

Synthesis and characterization of the Ru(II) complexes

The synthesis of the Ru(II) complexes was achieved in a 2-step process for **[Ru(DIP)$_2$(5-OHF)](PF$_6$)**, a 3-step process for **[Ru(DIP)$_2$(gen)](PF$_6$)** and **[Ru(DIP)$_2$(chr)](OTf)** and a 4-step process for **[Ru(DIP)$_2$(mor)](OTf)**, respectively (Scheme 1). Briefly, $RuCl_2(dmso)_4$[36], DIP and LiCl were refluxed in DMF to afford **Ru(DIP)$_2$Cl$_2$** in a 72% yield after precipitation with acetone.[37] **Ru(DIP)$_2$Cl$_2$** was then refluxed in a nitrogen atmosphere for 1.5-2 hours with the appropriate flavonoid in the presence of sodium ethoxide in dry ethanol. Complexes **[Ru(DIP)$_2$(5-OHF)](PF$_6$)** and **[Ru(DIP)$_2$(gen)](PF$_6$)** (25% and 13%, respectively) were obtained after precipitation with a large excess of NH_4PF_6 and further purification. Complexes **[Ru(DIP)$_2$(chr)](OTf)** and **[Ru(DIP)$_2$(mor)](OTf)** (16% and 35%, respectively) were obtained *via* a ruthenium triflate intermediate. Briefly, **Ru(DIP)$_2$Cl$_2$** and silver triflate were stirred to afford [Ru(DIP)$_2$(OTf)$_2$], and the appropriate flavonoid was added after filtration of AgCl in the presence of sodium ethoxide.

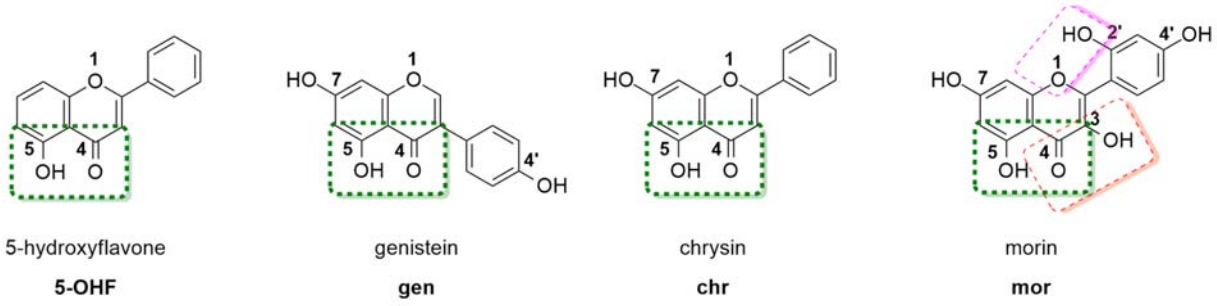

Figure 1. Chemical structures of flavonoids 5-hydroxyflavone, chrysin, genistein and morin.

Worthy of note, morin bears three possible coordination sites (Figure 1) and literature data suggests that the preferred binding site of metal ions to morin is the 3,4-*O*,*O* site.[38–41] Therefore, in order to

allow for comparison to the Ru(II) complexes of 5-OHF, genistein and chrysin, where the flavonoids coordinate *via* the 4,5-*O*,*O* site, the selective protection of the oxygen atoms at the 3, 7, 2' and 4' positions was necessary.

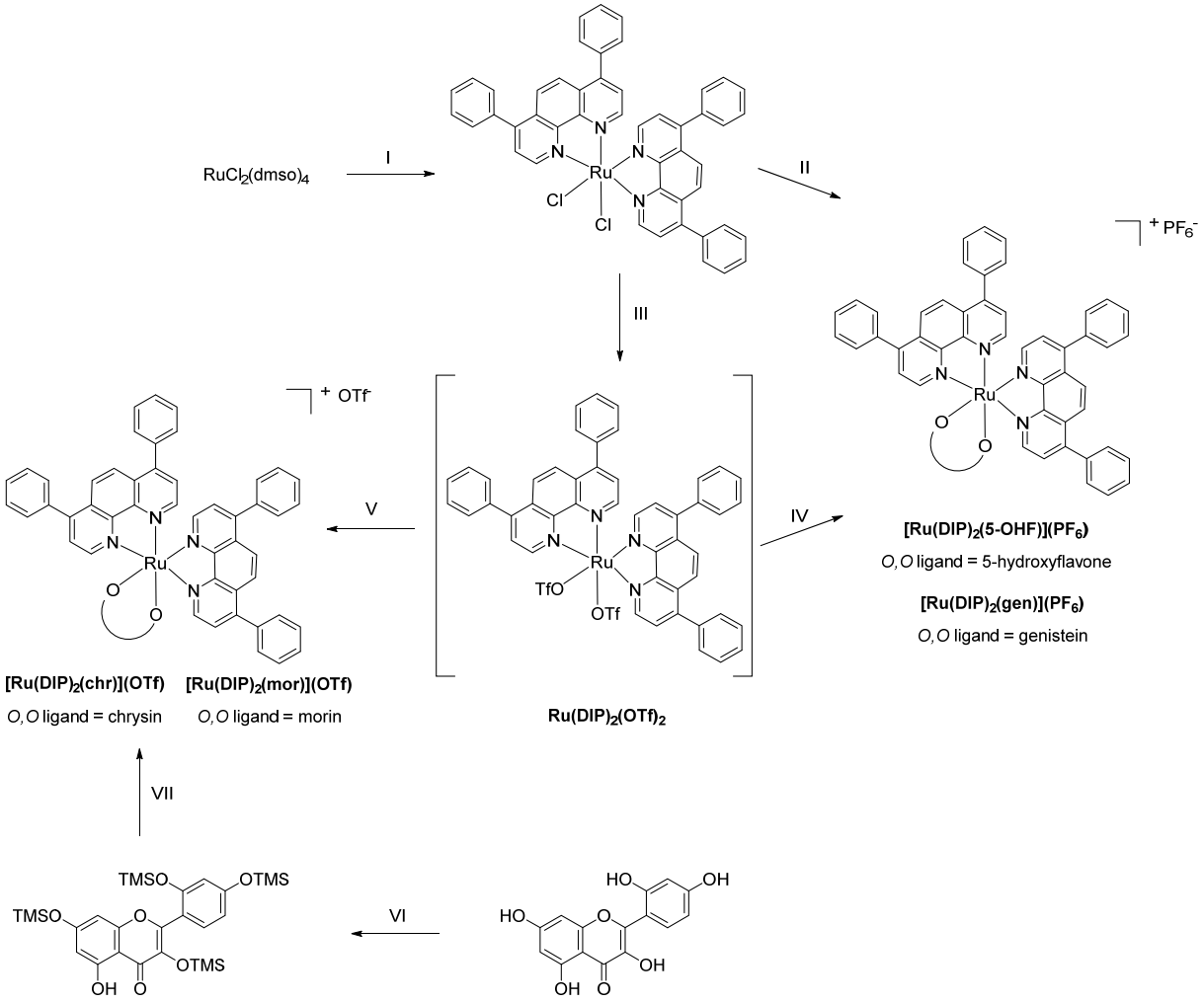

Scheme 1. Synthesis of complexes of the type $[Ru(DIP)_2(flv)]X$, where flv = flavonoid and X = counterion. I) DIP, LiCl, DMF, reflux, 24 h, 78%. II) (i) NaOH, 5-hydroxyflavone, ethanol, reflux, 2 h; (ii) NH_4PF_6, ethanol/H_2O (1:10), 25%. III) (i) silver triflate, ethanol, RT, 1h. IV) sodium ethoxide, genistein, ethanol, reflux, 2 h; (ii) NH_4PF_6, ethanol/H_2O (1:10), 13%. V) sodium ethoxide, chrysin, ethanol, reflux, 2 h, 16%. VI) NEt_3, TMSBr, THF, RT, 1h. VII) sodium ethoxide, $Ru(DIP)_2(OTf)_2$, ethanol, reflux, 2 h, 35%.

Therefore, the synthesis of **[Ru(DIP)$_2$(mor)](OTf)** involved an additional protection step shown in Scheme 1. Following a similar procedure to Qi *et al.*,[42] the selective protection at the 2', 4', 3 and 7 positions with trimethylsilyl (TMS) protecting group was achieved. The protection step was performed in the presence of triethylamine and TMS-Br in THF and, following an aqueous work-up, the protected morin was used in the complexation step without any further purification. The complexation reaction was performed as described above. Interestingly, during the course of the complexation reaction, the TMS protecting groups were hydrolysed, negating the need for a deprotection step. Following the successful synthesis of **[Ru(DIP)$_2$(mor)](OTf)**, coordination at the 4, 5-*O*,*O* site was confirmed by 1D and 2D NMR studies. It was noticed during the course of the NMR experiments that **[Ru(DIP)$_2$(mor)](OTf)** exists as a mixture of two isomers in solution. The second isomer is presumed to be the result of the morin binding *via* the 3,4-*O,O* site. The rate of isomerisation between the two isomers, however, is slow, with approximately 25% of the 3,4-*O,O* complex being visible by ^{1}H NMR after 5 days in solution (Figure S5). It should be noted that **[Ru(DIP)$_2$(mor)](OTf)** is stable if stored as a powder at -20 ^{o}C for over 6 months.

The identity of the compounds was confirmed by ESI-MS and NMR spectroscopy (Figures S1-S9) and their purity confirmed by microanalysis. All complexes are chiral and were isolated as a racemic mixture of Δ and Λ enantiomers. No attempt to obtain enantiopure complexes was made in this work. All four complexes are stable in the solid state and soluble in methanol, DCM, DMSO, DMF and moderately soluble in acetone, acetonitrile. Since the stability and aggregation of metal-based drug candidates is an important parameter, stability studies were undertaken.[43–45] Preliminary studies (Figures S10-S13) showed that **[Ru(DIP)$_2$(5-OHF)](PF$_6$)**, **[Ru(DIP)$_2$(gen)](PF$_6$)**, and **[Ru(DIP)$_2$(chr)](OTf)** are stable in DMSO over 5 days. The stability of **[Ru(DIP)$_2$(mor)](OTf)**, on the other hand, was tested in DMF due to the slower isomerisation

rate when compared to DMSO. Taking this into account, NMR analysis in DMF over 5 days shows no degradation of the product (Figure S13).

Cytotoxicity, cellular uptake and metabolic studies

The biological activity of the complexes was tested on MDA-MB-435S (human, melanoma), FaDU (human, pharynx carcinoma), MCF-7 (human, ductal carcinoma), U87 (human, glioblastoma), RPE-1 (human, normal retinal pigmented epithelium) and HEK 293 (human embryonic kidney) cell lines using a fluorometric cell viability assay.[46] Cisplatin and doxorubicin were tested in the same conditions as positive controls.[47,48] **$Ru(DIP)_2Cl_2$** as well as the flavonoids 5-hydroxyflavone, genistein, chrysin and morin were used as additional controls. The IC_{50} (half maximal inhibitory concentration) values obtained in this study are reported in Table 1 (all cytotoxicity graphs are available in Figure S14).

Table 1. IC_{50} values for flavonoid ligands, cisplatin, doxorubicin, **$[Ru(DIP)_2(5\text{-}OHF)](PF_6)$**, **$[Ru(DIP)_2(gen)](PF_6)$**, **$[Ru(DIP)_2(chr)](OTf)$**, **$[Ru(DIP)_2(mor)](OTf)$,** and **$Ru(DIP)_2Cl_2$** in different cell lines (48 h treatment).

Compounds	**IC_{50} (µM)**					
	MCF-7	FaDU	MDA-MB-435S	U87	RPE-1	HEK293
5-Hydroxyflavone	>100	>100	>100	>100	>100	>100
Genistein	>100	>100	>100	>100	>100	75.85 ± 0.84
Chrysin	62.59 ± 3.23	95.06 ± 11.55	79.37 ± 8.13	91.14 ± 13.76	>100	26.80 ± 2.79
Morin	>100	>100	>100	>100	>100	>100

Cisplatin	19.69 ± 1.63	5.17 ± 0.21	17.62 ± 0.54	6.94 ± 0.46	39.9 ± 9.14	2.27 ± 0.67
Doxorubicin	9.39 ± 1.37	1.55 ± 0.18	5.55 ± 1.37	0.59 ± 0.03	14.9 ± 1.31	0.21 ± 0.03
$Ru(DIP)_2Cl_2$	>50	>50	27.73 ± 5.33	25.59 ± 0.29	3.13 ± 0.28	12.11 ± 1.30
$[Ru(DIP)_2(5\text{-}OHF)](PF_6)$	>50	38.21 ± 5.22	24.48 ± 1.92	30.72 ± 1.48	19.72 ± 8.23	26.46 ± 3.20
$[Ru(DIP)_2(gen)](PF_6)$	16.67 ± 3.93	5.21 ± 0.73	2.64 ± 0.43	5.21 ± 1.74	2.36 ± 0.77	0.72 ± 0.10
$[Ru(DIP)_2(chr)](OTf)$	>50	>50	27.73 ± 5.33	25.59 ± 0.29	23.21 ± 8.08	33.02 ± 3.25
$[Ru(DIP)_2(mor)](OTf)$	>50	>50	>50	>50	>50	>50

The literature cites good to excellent cytotoxic activity for other 5-hydroxyflavone, chrysin and morin metal complexes,[41,49–52] results that prompted us to the design of these compounds. Worthy of note, complexes of morin (bound *via* the 3,4-*O,O* site) and chrysin bearing a Ru(II) polypyridyl scaffold have been previously reported. Their cytotoxic activity was studied on HeLa (cervical carcinoma), SW620 (colorectal adenocarcinoma, metastatic), HepG2 (hepatocellular carcinoma) and MCF-7 cell lines with IC_{50} values ranging from 7.64 to >100 μM.[41] **$[Ru(DIP)_2(mor)](OTf)$**, however, was found to be essentially non-toxic, with IC_{50} values above 50 μM in all cell lines tested, while **$[Ru(DIP)_2(5\text{-}OHF)](PF_6)$** and **$[Ru(DIP)_2(chr)](OTf)$** exerted moderate toxicity towards some of the cell lines tested. Interestingly, the most promising complex identified in this study is the complex bearing the flavonoid genistein, (**$[Ru(DIP)_2(gen)](PF_6)$**), with IC_{50} values comparable to those of both cisplatin and doxorubicin. Genistein is considered a suitable lead for anticancer drug development and derivatives have been synthesised in order to enhance its cytotoxic activity. [53–57] It should be stated that among all chemical derivatives of genistein, scarce data exists regarding its metal complexes. For instance, a homoleptic copper (II) genistein complex

was reported to enhance the cytotoxic activity of the ligand against four cancer cell lines, including 518A2 melanoma and MCF-7/Topo breast carcinoma cell lines.[52] Unfortunately, **[Ru(DIP)$_2$(gen)](PF$_6$)** exerted no selectivity between cancerous and non-cancerous cell lines with comparable IC_{50} values. However, this drawback is commonly faced in medicinal chemistry and could be improved by the introduction of a targeting moiety.

[Ru(DIP)$_2$(gen)](PF$_6$) showed good activity towards the MDA-MB-435S cell line, with an IC_{50} of 2.64 μM. Currently, this cell line is identified as a melanoma cell line, which derives from the pleural effusion of a 31-year-old female with metastatic, ductal adenocarcinoma of the breast and considered still valuable for the study of metastasis.[58,59] The lower activity expressed by the complex towards the MCF-7 cell line (IC_{50}=16.67 μM) led us to study the cellular uptake and mechanism of uptake of this complex in two different cell lines derived from breast tissue. In these experiments, cells were treated with 5 μM of **[Ru(DIP)$_2$(gen)](PF$_6$)** for 2 h and the metal content was analysed *via* inductively coupled plasma mass spectrometry (ICP-MS). Cisplatin and **Ru(DIP)$_2$Cl$_2$** were tested in the same conditions as controls. The viability of the cells after the 2 h treatment was additionally tested, confirming that the acquired results were obtained from living cells (Figure S14). Figure 2a shows that the cellular uptake is much lower for the MCF-7 cell line when compared to MDA-MB-435S for all the tested compounds. Interestingly, **Ru(DIP)$_2$Cl$_2$** accumulates more in MDA-MB-435S compared to **[Ru(DIP)$_2$(gen)](PF$_6$)**, in the same cell line, but shows lower cytotoxicity than the flavonoid complex. This observation can be rationalised by the explanation provided by Policar *et al.* in 2014 where they state that IC_{50} is a resultant value of cellular uptake, interaction with cellular target and its intrinsic toxicity.[60] Therefore, one could argue that the higher activity expressed by **[Ru(DIP)$_2$(gen)](PF$_6$)** towards MDA-MB-435S when compared to MCF-7 cells, comes as a consequence of its higher cellular uptake. To understand the

kinetics of the tested compounds in the chosen cell lines, we have performed time-dependent accumulation experiments. Ruthenium and platinum contents in treated cells were measured by ICP-MS after 2 h, 12 h, 24 h and 48 h. In this analysis, the concentration of the tested compounds was decreased to 1 μM to reduce cell loss during the experiment. Figures 2b and 2c show the changes in cellular accumulation in the two cell lines tested. The obtained results confirm previous conclusions that all tested compounds accumulate more in the MDA-MB-435S cell line than in MCF-7 cells. After 24 h incubation time, a similar uptake of **$Ru(DIP)_2Cl_2$** and **$[Ru(DIP)_2(gen)](PF_6)$** was found in MDA-MB-435S (~ 30 ng of metal in 10^6 cells) in comparison with cisplatin (~ 4 ng of metal in 10^6 cells). On the other hand, **$[Ru(DIP)_2(gen)](PF_6)$** accumulates much more in MCF-7 cells than the two other compounds after 24 h (~ 2 ng of metal in 10^6 cells as compared to ~ 1 ng) and 48 h (~ 5 ng of metal in 10^6 cells compared to ~ 1 ng). Notably, there is a discrepancy between the amount of metal detected in the total accumulation and the time dependent accumulation experiments in both cell lines at the 2 h time point (shown in Figures 2a, 2b and 2c). This can be explained by the different mechanisms of uptake of the Ru complexes (see below) and the availability of the complexes in cellular media (5 times lower concentration of the compounds in the time dependent experiments).

To understand the nature of the mechanism of uptake (passive or active) of the tested complexes, cells were pre-treated with various inhibitors or kept at different temperatures. A temperature of 4 ºC was used to slow down passive diffusion, as well as active transportation. To block cellular metabolism, pre-treatments with ATP production inhibitors 2-deoxy-*D*-glucose and oligomycin were performed. Chloroquine or ammonium chloride (NH_4Cl) impede endocytic pathways and tetraethylammonium chloride stops the cation transporters. Following pre-treatments, cells were

incubated with **[Ru(DIP)$_2$(gen)](PF$_6$)** or **Ru(DIP)$_2$Cl$_2$** (2 h, 5 μM) and subsequently analysed *via* ICP-MS (Figures 2d and 2e).

Inhibition of active uptake mechanisms did not significantly perturb accumulation of **[Ru(DIP)$_2$(gen)](PF$_6$)** in both cell lines tested, demonstrating that the mechanism responsible for its accumulation is energy independent (passive). On the other hand, **Ru(DIP)$_2$Cl$_2$** is taken up *via* a passive mechanism by the MCF-7 cell line and an active mechanism by the MDA-MB-435S cell line. As shown for other similar ruthenium complexes, this observation indicates that slight changes in lipophilic properties and structure play a decisive role in the cellular uptake of Ru(II) polypyridyl complexes.[61–63]

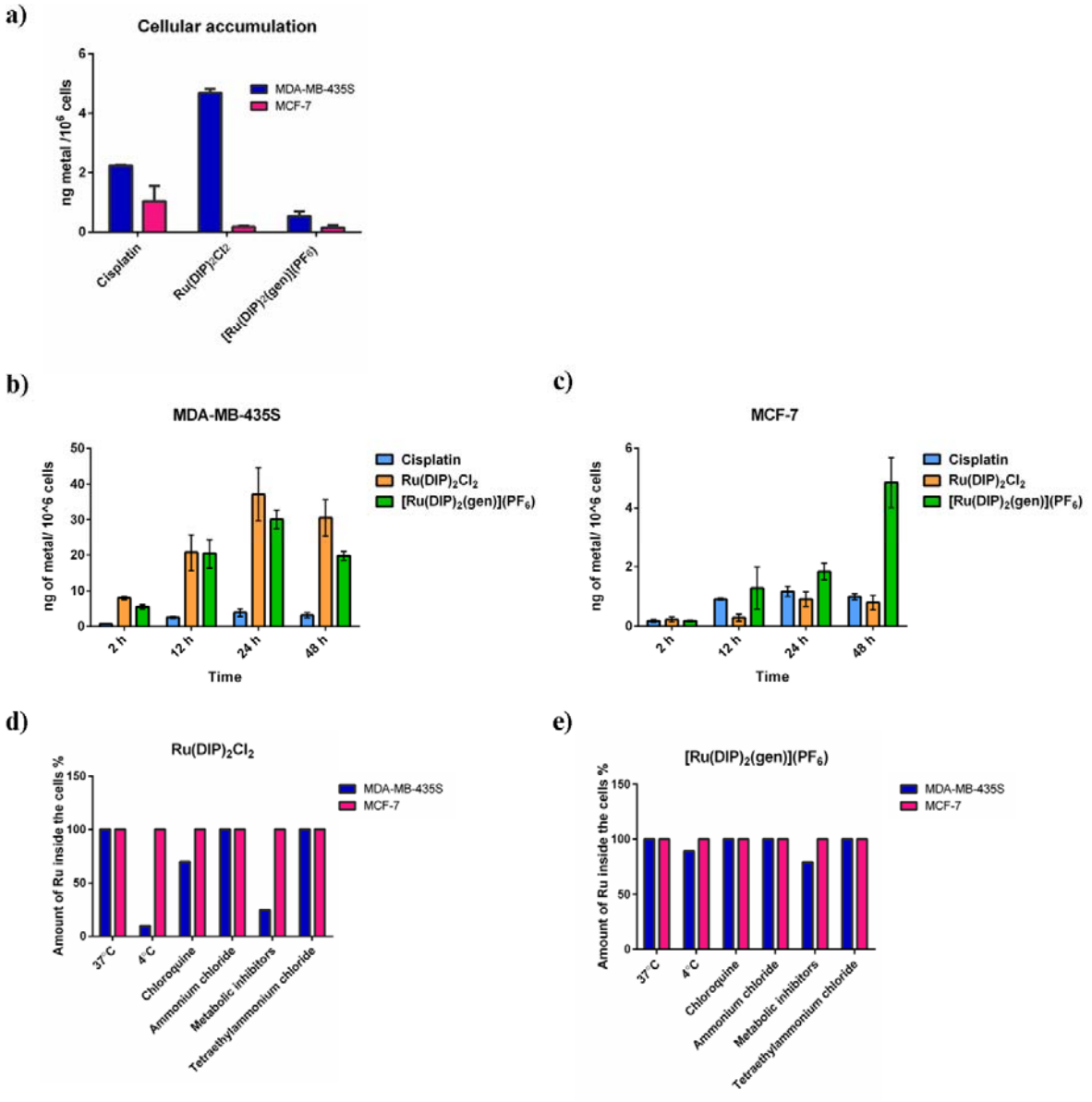

Figure 2. ICP-MS data of cellular uptake of tested compounds in MDA-MB-435S and MCF-7 cell lines. (a) Total cellular accumulation (2 h treatment, 5 μM) (b) Time-dependent cellular accumulation in MDA-MB-435S cell line (c) Time-dependent cellular accumulation in MCF-7 cell line (d) Mechanism of cellular uptake of **$Ru(DIP)_2Cl_2$** in tested cell lines (2 h treatment, 5 μM) (e) Mechanism of cellular uptake of **$[Ru(DIP)_2(gen)](PF_6)$** in tested cell lines (2 h treatment,

5 μM). Data of (a), (d) and (e) is presented as the mean ± SD of at least 3 technical replicates. Data of (b) and (c) is presented as the mean ± SD of at least 3 biological replicates

To better understand the effect of the flavonoid complex of interest on the cellular metabolism of MDA-MB-435S cells, a Seahorse XF Analyser was used. This device allows for the real time measurement of the oxygen consumption rate (OCR) and extracellular acidification rate (ECAR) in cells. Firstly, the influence on the oxidative phosphorylation was measured. As shown in Figures 3a and S15, 24 h treatment with flavonoid complex **[Ru(DIP)$_2$(gen)](PF$_6$)** and its precursor **Ru(DIP)$_2$Cl$_2$** strongly inhibit mitochondrial respiration. Cells do not respond to the oligomycin injection, which inhibits ATP synthase,[64] nor to the FCCP which will interfere with the mitochondrial membrane proton gradient.[65] ATP production, as well as spare respiratory capacity (calculated as the difference between maximal and basal respiration), are extremely low, further confirming non-functioning mitochondria in treated MDA-MB-435S cells.

Next, the effect on the glycolysis process was investigated. Figures 2b and S16 show interesting differences between the modes of action of **[Ru(DIP)$_2$(gen)](PF$_6$)** and **Ru(DIP)$_2$Cl$_2$**. During the glycolysis stress test the first injection is made with a saturated solution of glucose. This treatment should trigger the glycolysis process in cells and consequently lead to higher ECAR. Surprisingly, MDA-MB-435S cells treated with **[Ru(DIP)$_2$(gen)](PF$_6$)** showed no increase in ECAR values following injection of the saturated glucose solution. This observation is a clear indication of the impaired glycolytic process. On the other hand, cells treated with **Ru(DIP)$_2$Cl$_2$** showed similar glycolysis levels when compared to those of the untreated cells. This suggests that the cytosolic process of ATP production is impaired in **[Ru(DIP)$_2$(gen)](PF$_6$)** treated cells, but not in those treated with **Ru(DIP)$_2$Cl$_2$**. Furthermore, the lack of response to the oligomycin injection in cells treated with both complexes, agrees with the results obtained *via* the mito stress test, which

suggests non-functioning mitochondria after both treatments. Interestingly, the complexes **[Ru(DIP)$_2$(sq)](PF$_6$)**, **[Ru(DIP)$_2$(mal)](PF$_6$)** and **[Ru(DIP)$_2$(3-methoxysq)](PF$_6$),** recently reported by our group, also showed impaired mitochondrial function but did not show any effect on the glycolysis process.[66–68] This illustrates how subtle structural changes in the complexes bearing the same Ru(DIP)$_2$ core but different dioxo ligands, can result in significantly different behaviour of the complexes in living cells.

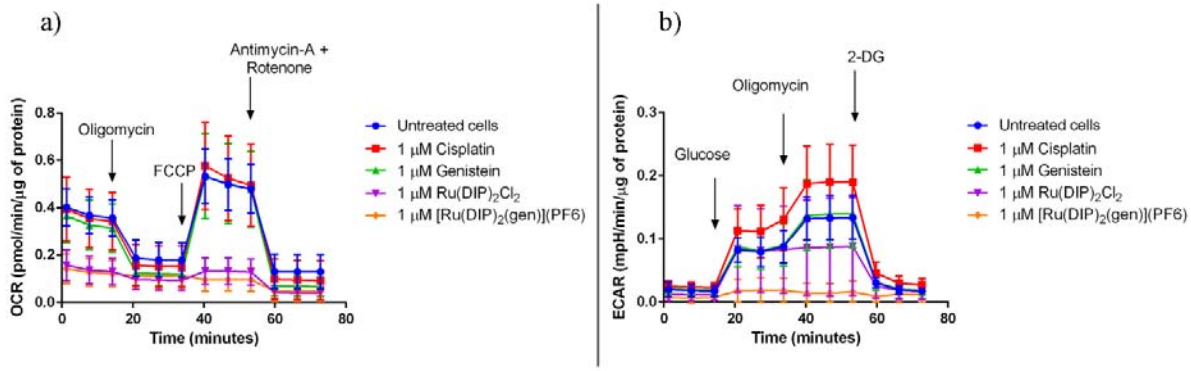

Figure 3. a) Mito Stress Test profile in MDA-MB-435S cells after 24 h treatment. Oxygen consumption rate changes after treatment with specific electron transport chain inhibitors. Oligomycin (inhibitor of ATP synthase (complex V)), FCCP (uncoupling agent), antimycin-A (complex III inhibitor) and rotenone (complex I inhibitor). b) Glycolysis Stress Test profile in MDA-MB-435S cells after 24 h treatment. Extracellular acidification rate that corresponds to the glycolysis process changes after treatment with glucose (basal level of glycolysis in cells), oligomycin (inhibitor of ATP synthase (complex V) - mitochondria inhibition), 2-deoxyglucose (analogue of glucose that inhibits glycolytic pathway).

Conclusions

Briefly, four monocationic Ru(II) polypyridyl complexes with the general formula $[Ru(DIP)_2flv]X$ have been synthesised. The cytotoxicity of these complexes was tested against different cancerous and healthy cell lines and the most promising compound identified is **$[Ru(DIP)_2(gen)](PF_6)$** with cytotoxicity comparable to that of cisplatin and doxorubicin. The complex displayed good activity towards the MDA-MB-435S cell line (IC_{50} = 2.64 μM), a melanoma cell line derived from the pleural effusion of a female with metastatic breast adenocarcinoma, used for the study of metastasis. Interestingly, genistein was not cytotoxic (IC_{50} > 100 μM) and the precursor, **$Ru(DIP)_2Cl_2$**, was only moderately active (IC_{50} = 27.73 μM). **$[Ru(DIP)_2(gen)](PF_6)$** was found to be taken up more efficiently by MDA-MB-435S cell lines than MCF-7, a commonly used breast cancer cell line, in both cases *via* a passive transportation mechanism. Further metabolic studies in the MDA-MB-435S cell line revealed that **$[Ru(DIP)_2(gen)](PF_6)$** not only inhibits mitochondrial respiration, but also interferes with the cytosolic glycolysis process in comparison to **$Ru(DIP)_2Cl_2$**. This result suggests that addition of the flavonoid moiety changes the behaviour of the complex in living cells and allows for a more complex mode of action, leading to cell death. Therefore, we consider **$[Ru(DIP)_2(gen)](PF_6)$** to be a suitable candidate for further studies, which will aim to identify the cellular targets of the complex and possible interactions with protein transporters. Since the current treatment of advanced melanoma provides modest results, this work may open new opportunities in the search for chemopreventive and/or chemotherapeutic agents for human cancers, especially melanoma.

Experimental Section

Materials

All chemicals were either of reagent or analytical grade and used as purchased from commercial sources without additional purification. Ruthenium trichloride hydrate was provided by I^2CNS, 4,7-diphenyl-1,10-phenanthroline, lithium chloride (anhydrous, 99%), the flavonoids and tetrabutylammonium hexafluorophosphate were provided by Sigma-Aldrich. All solvents were purchased of analytical, or HPLC grade. When necessary, solvents were degassed by purging with dry, oxygen-free nitrogen for at least 30 minutes before use. Preparative thin layer chromatography (TLC) glass plates (Analtech, Sigma-Aldrich, Steinheim, Germany, 20 cm × 20 cm; 1500 μm thickness).

Instrumentation and methods

Amber glass or clear glassware wrapped in tin foil were used when protection from the light was necessary. Schlenk glassware and a vacuum line were employed when reactions sensitive to moisture/ oxygen had to be performed under a nitrogen atmosphere. Thin layer chromatography (TLC) was performed using silica gel 60 F-254 (Merck) plates with detection of spots being achieved by exposure to UV light. Eluent mixtures are expressed as volume to volume (v/v) ratios. ^1H and ^{13}C NMR spectra were measured on Bruker Avance III HD 400 MHz or Bruker Avance Neo 500 MHz spectrometers using the signal of the deuterated solvent as an internal standard.[69] The chemical shifts δ are reported in ppm (parts per million) relative to tetramethylsilane (TMS) or signals from the residual protons of deuterated solvents. The following abbreviations were used to designate multiplicities: s = singlet, d = doublet, app t = apparent triplet, m = multiplet, dd = double-doublet, br = broad. Chemical shifts were expressed in ppm. ESI experiments were carried

out using a 6470 Triple Quad (Agilent Technologies). Elemental analysis was performed at Science Centre, London Metropolitan University using Thermo Fisher (Carlo Erba) Flash 2000 Elemental Analyser, configured for %CHN. IR spectra were recorded with a SpectrumTwo FTIR Spectrometer (Perkin–Elmer) equipped with a Specac Golden GateTM ATR (attenuated total reflection) accessory; applied as neat samples; $1/\lambda$ in cm^{-1}.

Synthesis and characterization

$RuCl_2(dmso)_4$

$RuCl_2(dmso)_4$ was synthesised following an adapted literature procedure.[36] Spectroscopic data were in agreement with the literature.[36]

$Ru(DIP)_2Cl_2$

$Ru(DIP)_2Cl_2$ was synthesised following an adapted literature procedure.[36] Spectroscopic data were in agreement with the literature.[37,66]

$[Ru(DIP)_2(5\text{-}OHF)](PF_6)$

$Ru(DIP)_2Cl_2$ (0.20 g, 0.24 mmol) and aq. NaOH (0.38 mL, 1 M) were dissolved in ethanol (20 mL). The solution was degassed for 20 min and 5-hydroxyflavone (0.09 g, 0.38 mmol) was added. The resulting mixture was heated to reflux for 1.5 h under a N_2 atmosphere and protected from light. The mixture was cooled to RT, while still protected from light, and the solvent was removed under vacuum. The residual solid was redissolved in ethanol (10 mL), and H_2O (100 mL) and NH_4PF_6 (1.00 g, 6.13 mmol) were added. The precipitate formed was filtered, washed with H_2O (3 × 50 mL) and Et_2O (3 × 50 mL) and collected. The solid with Et_2O (10 mL) and then heptane (10 mL), was sonicated for 10 min and then centrifuged. This procedure was repeated three times for each solvent. The solid was collected with DCM and dried under vacuum to deliver

[Ru(DIP)$_2$(5-OHF)](PF$_6$) (0.07 g, 0.061 mmol, 25 % yield) as a purple solid. ^{1}H NMR (400 MHz, CD_2Cl_2): δ/ppm = 9.54 (d, *J* = 5.5 Hz, 1H), 9.38 (d, *J* = 5.5 Hz, 1H), 8.27 (d, *J* = 8.7 Hz, 2H), 8.21 – 8.16 (m, 3H), 8.11 (d, *J* = 5.5 Hz, 1H), 7.96 (dd, *J* = 9.4, 5.5 Hz, 2H), 7.92 – 7.89 (m, 2H), 7.78 – 7.50 (m, 23H), 7.42 (dd, *J* = 10.5, 5.5 Hz, 2H), 7.35 (app t, *J* = 8.3 Hz, 1H), 6.74 (s, 1H), 6.65 (dd, *J* = 11.6, 8.3 Hz, 2H); ^{13}C NMR (125 MHz, CD_2Cl_2): δ/ppm = 179.9, 168.1, 160.0, 158.1, 153.5, 153.1, 151.6, 151.1, 151.0, 150.2, 149.8, 149.6, 148.0, 147.7, 146.3, 146.2, 136.2, 136.2, 136.0, 136.0, 134.3, 131.8, 131.0, 129.9, 129.9, 129.7, 129.7, 129.6, 129.5, 129.5, 129.4, 129.2, 129.1, 128.6, 128.6, 128.4, 126.0, 125.9, 125.8, 125.7, 125.6, 125.4, 124.7, 124.5, 118.3, 113.0, 105.9, 100.3. MS (ESI+): m/z 1003.22 $[M]^+$. Elemental Analysis: calcd. for $C_{63}H_{41}F_6N_4O_3PRu$ = C, 65.91; H, 3.60; N, 4.88. Found = C, 65.70; H, 3.58; N, 4.55.

[Ru(DIP)$_2$(gen)](PF$_6$)

$Ru(DIP)_2Cl_2$ (0.20 g, 0.24 mmol) was dissolved in ethanol (20 mL). The solution was degassed for 20 min and silver triflate (0.13 g, 0.52 mmol) was added. The mixture was stirred at RT for 1 h protected from light, under a N_2 atmosphere. The crude reaction mixture was filtered and the filtrate was degassed for 20 min. To the degassed solution, genistein (0.10 g, 0.38 mmol) and an ethanolic solution of sodium ethoxide (21%, 285 μL) were added. The mixture was heated to reflux for 2 h under N_2 atmosphere whilst protected from light. The mixture was cooled to RT and the solvent was removed under vacuum. The residual solid was dissolved in ethanol (10 mL), and H_2O (100 mL) and NH_4PF_6 (1.00 g, 6.13 mmol) were added. The precipitate which formed was filtered and washed with H_2O (3 x 50 mL), heptane (3 x 50 mL) and Et_2O (2 x 50 mL). The solid was collected with DCM and dried under vacuum to deliver the crude product. Purification was achieved *via* preparative TLC (DCM/ethylacetate/methanol 79/20/1). The product was collected

from the prep TLC with methanol and the solvent was subsequently removed under reduced pressure. The solid with Et_2O (10 mL) and then heptane (10 mL), was sonicated for 10 min and then centrifuged. This procedure was repeated three times for each solvent. The solid was collected with DCM and dried under vacuum to deliver **[Ru(DIP)$_2$(gen)](PF$_6$)** (0.04 g, 0.033 mmol, 14%) as a deep purple solid. ^{1}H NMR (400 MHz, CD_3OD): δ/ppm = 9.59 (d, *J* = 5.5 Hz, 1H), 9.21 (d, *J* = 5.5 Hz, 1H), 8.42 (d, *J* = 5.5 Hz, 1H), 8.28 (dd, *J* = 9.4, 1.4 Hz, 2H), 8.20 (dd, *J* = 9.4, 3.7 Hz, 2H), 8.10 (dd, *J* = 5.5, 2.3 Hz, 2H), 8.00 (d, *J* = 5.5 Hz, 1H), 7.82 – 7.73 (m, 5H), 7.72 – 7.53 (m, 18H), 7.50 (d, *J* = 5.5 Hz, 1H), 7.38 (d, *J* = 5.5 Hz, 1H), 6.50 (d, *J* = 8.7 Hz, 2H), 6.26 (d, *J* = 8.7 Hz, 2H), 6.10 (s, 1H); ^{13}C NMR (125 MHz, CD_3OD): δ/ppm = 178.2, 169.5, 165.5, 160.9, 158.1, 155.2, 155.1, 153.0, 152.7, 152.6, 152.1, 151.2, 150.9, 150.9, 149.6, 149.1, 147.8, 147.5, 137.7, 137.6, 137.6, 137.5 131.1, 131.1, 131.0, 130.8, 130.5, 130.4, 130.3, 130.2, 130.1, 130.1, 130.1, 129.7, 129.7, 129.6, 129.5, 126.9, 126.8, 126.7, 126.7, 126.6 125.9, 125.8, 124.2, 123.6, 115.3, 109.3, 92.4, 58.3. MS (ESI+): m/z 1035.5 $[M]^+$. Elemental Analysis: calcd. for $C_{63}H_{41}F_6N_4O_5PRu$ = C, 64.12; H, 3.50; N, 4.75. Found = C, 64.51; H, 3.45; N, 4.48.

[Ru(DIP)$_2$(chr)](OTf)·4H$_2$O

$Ru(DIP)_2Cl_2$ (0.50 g, 0.60 mmol) was dissolved in ethanol (30 mL). The solution was degassed for 20 min and silver triflate (0.34 g, 1.32 mmol) was added. The mixture was stirred at RT for 1 h protected from light, under a N_2 atmosphere. The crude reaction mixture was filtered and the filtrate was degassed for 20 min before chrysin (0.24 g, 0.96 mmol) and an ethanolic solution of sodium ethoxide (21%, 717 μL) were added. The mixture was heated to reflux for 2 h under N_2 atmosphere and protected from light. The mixture was cooled to RT, while still protected from light, and the solvent was removed under vacuum. The residual solid was collected in DCM (20

mL) and filtered through celite. The solvent was removed under vacuum to deliver the crude product. Purification was achieved *via* preparative TLC (DCM/ethylacetate/methanol 79/20/1). The product was collected from the prep TLC with methanol and the solvent was subsequently removed under reduced pressure. The solid with Et_2O (10 mL) and then heptane (10 mL), was sonicated for 10 min and then centrifuged. This procedure was repeated three times for each solvent. The solid was collected with DCM and dried under vacuum to afford **[Ru(DIP)$_2$(chr)](OTf)** (0.12 g, 0.09 mmol, 16% yield) as a deep purple solid. ^{1}H NMR (400 MHz, CD_2Cl_2-d_2): δ/ppm = 9.56 (d, J = 5.5 Hz, 1H), 9.32 (d, J = 5.5 Hz, 1H), 8.20 – 8.09 (m, 4H), 8.09 – 7.99 (m, 2H), 7.84 – 7.80 (m, 2H), 7.76 (d, J = 7.3 Hz, 2H), 7.69 – 7.36 (m, 24H), 7.34 (d, J = 5.5 Hz, 1H), 7.28 (d, J = 5.5 Hz, 1H), 6.48 (s, 1H), 6.17 (br d, J = 2.2 Hz, 1H), 6.04 (br d, J = 2.2 Hz, 1H). ^{13}C NMR (125 MHz, CD_2Cl_2): δ/ppm = 178.2, 169.1, 160.0, 159.4, 153.7, 153.4, 152.3, 152.0, 151.6, 150.7, 150.2, 150.2, 147.9, 147.7, 146.3, 146.2, 136.9, 136.8, 136.7, 136.6, 131.8, 131.7, 130.4, 130.4, 130.2, 130.1, 129.9, 129.8, 129.7, 129.6, 129.6, 129.5, 129.0, 129.0, 128.8, 126.3, 126.2, 126.1, 125.8, 125.1, 107.7, 105.5, 104.6, 92.3. MS (ESI+): m/z 1019.6 $[M]^+$, (ESI-): m/z 149.2 [OTf]. Elemental Analysis: calcd. for $C_{64}H_{49}F_3N_4O_{11}RuS$ = C, 61.97; H, 3.99; N, 4.51. Found = C, 62.09; H, 3.93; N, 4.28.

[Ru(DIP)$_2$(mor)](OTf)

A. Morin (0.56 g, 1.85 mmol) was suspended in dry tetrahydrofuran (50 mL) and triethylamine (1.55 mL, 11.1 mmol) was added. The mixture was stirred at RT under a N_2 atmosphere for 15 minutes before TMS-Br (1.47 mL, 11.1 mmol) was added. The mixture was stirred at RT under a N_2 atmosphere for 2.5 h before being added to a separating funnel. H_2O (50 mL) was added and

the product was extracted in DCM and dried on Na_2SO_4. The solvent was removed under vacuum to yield the crude product *A*.

B. $Ru(DIP)_2Cl_2$ (0.83 g, 1.00 mmol) was dissolved in ethanol (50 mL). The solution was degassed for 20 min and silver triflate (0.56 g, 2.20 mmol) was added. The mixture was stirred at RT for 1 h protected from light, under a N_2 atmosphere. The crude reaction mixture was filtered and the filtrate was degassed for 20 min before product *A* and an ethanolic solution of sodium ethoxide (21%, 750 µL) were added. The mixture was heated to reflux for 2 h under N_2 atmosphere and protected from light. The mixture was cooled to RT, while still protected from light, and the solvent was removed under vacuum. The residual solid was collected in DCM (20 mL) and filtered through celite. The solvent was removed under vacuum to deliver the crude product. Purification was achieved *via* preparative TLC (DCM/ethylacetate/methanol 79/20/1). The product was collected from the prep TLC with methanol and the solvent was subsequently removed under reduced pressure. The solid with Et_2O (10 mL) and then heptane (10 mL), was sonicated for 10 min and then centrifuged. This procedure was repeated three times for each solvent. The solid was collected with DCM and dried under vacuum to afford **[Ru(DIP)$_2$(mor)](OTf)** (0.42 g, 0.35 mmol, 35% yield) as a deep purple solid. ^{1}H NMR (400 MHz, DMF-d_7): δ/ppm = 11.85 (s, 1H), 9.73 (dd, J = 10.1, 5.5 Hz, 2H), 8.53 (d, J = 5.5 Hz, 1H), 8.45 (d, J = 5.5 Hz, 1H), 8.42 – 8.20 (m, 7H), 7.93 – 7.49 (m, 25H), 6.45 (dd, J = 8.7, 2.4 Hz, 1H), 6.06 (d, J = 2.4 Hz, 1H), 5.99 (s, 1H), 5.76 (s, 1H). ^{13}C NMR (125 MHz, DMF-d_7): δ/ppm = 158.9, 158.0, 155.0, 154.7, 151.9, 151.8, 151.8, 151.5, 149.7, 149.6, 147.3, 147.0, 145.7, 145.5, 143.3, 136.4, 136.1, 136.0, 130.3, 130.2, 130.0, 129.4, 129.3, 129.2, 129.1, 128.8, 128.2, 128.0, 126.4, 126.3, 125.9, 125.9, 125.8, 125.7, 125.1, 125.0, 112.5, 108.0, 104.9, 95.7. MS (ESI+): m/z 1067.9 $[M]^+$, (ESI-): m/z 149.3 $[OTf]^-$. Elemental

Analysis: calcd. for $C_{64}H_{41}F_3N_4O_{10}RuS$ = C, 63.20; H, 3.40; N, 4.60. Found = C, 62.77; H, 3.33; N, 4.45.

Stability studies

The stability in DMSO-d_6 or DMF-d_7 at room temperature was assessed by ^{1}H NMR over 96 h.

Cytotoxicity assay using a 2D cellular model

Cytotoxicity of **[Ru(DIP)$_2$(5-OHF)](PF$_6$)**, **[Ru(DIP)$_2$(gen)](PF$_6$)**, **[Ru(DIP)$_2$(chr)](OTf)**, **[Ru(DIP)$_2$(mor)](OTf)**, **Ru(DIP)$_2$Cl$_2$**, cisplatin and doxorubicin was assessed by a fluorometric cell viability assay using Resazurin (ACROS Organics). Briefly, cells were seeded in triplicate in 96-well plates at a density of 4×10^3 cells/well in 100 µL. After 24 h, cells were treated with increasing concentrations of the ruthenium complexes. Dilutions were prepared as follows: 0.250 mM stock in DMSO (**[Ru(DIP)$_2$(5-OHF)](PF$_6$)**, **[Ru(DIP)$_2$(gen)](PF$_6$)**, **[Ru(DIP)$_2$(chr)](OTf)**) or DMF (**[Ru(DIP)$_2$(mor)](OTf)**, **Ru(DIP)$_2$Cl$_2$**, which were further diluted to 100 µM in cell media. After 48 h incubation, the medium was removed and 100 µL of complete medium containing resazurin (0.2 mg/mL final concentration) was added. After 4 h of incubation at 37 °C, the fluorescence signal of resorufin product was read (ex: 540 nm em: 590 nm) in a SpectraMax M5 microplate Reader. IC_{50} values were then calculated using GraphPad Prism software.

GraphPad Prism calculations of IC_{50} values

XY analysis with three replicate values in side by side sub-columns were chosen. Inserted raw data obtained from SpectraMax M5 microplate reader was treated as follows: X values were transformed into logarithm; data was normalised to the lowest Y value. Data was then analysed with XY analysis "Nonlinear regression (curve fit)" then "log(inhibitor) vs. normalized response".

Cytotoxicity assay using a 2D cellular model f (2 h incubation)

Cytotoxicity of **[Ru(DIP)$_2$(gen)](PF$_6$)** and cisplatin was assessed by a fluorometric cell viability assay using Resazurin (ACROS Organics). Briefly, cells were seeded in triplicate in 96-well plates at a density of 4×10^3 cells/well in 100 µL. After 24 h, cells were treated with increasing concentrations of the complexes. Dilutions were prepared as described in the section "Cytotoxicity assay using a 2D cellular model". After 2 h incubation, the medium was removed and 100 µL of complete medium containing resazurin (0.2 mg/mL final concentration) was added. After 4 h of incubation at 37 °C, the fluorescence signal of resorufin product was read (ex: 540 nm em: 590 nm) in a SpectraMax M5 microplate Reader. IC_{50} values were then calculated using GraphPad Prism software as stated before.

Sample Preparation for cellular uptake

MDA-MB-435S and MCF-7 cells were seeded at a density of 2×10^6 in 10 cm plates. Next day, cells were treated with 5 µM concentration of **[Ru(DIP)$_2$(gen)](PF$_6$)**, **Ru(DIP)$_2$Cl$_2$** or cisplatin. Dilutions were prepared as described in the section "Cytotoxicity assay using a 2D cellular model". After 2 h, cells were washed, collected, counted and snap frozen in liquid nitrogen and stored at -20 ºC. ICP-MS samples were prepared as follows: samples were digested using 70% nitric acid (1 mL, 60 ºC, overnight). Samples were then further diluted 1:100 (1% HCl solution in MQ water) and analysed using ICP-MS.

Sample preparation for studies on the mechanism of cellular uptake

Samples were prepared as previously reported.[66] Briefly, MDA-MB-435S and MCF-7 cells were seeded at a density of 2×10^6 in 10 cm dishes and were pre-treated the following day with the corresponding inhibitors or kept at a specific temperature for 1 h. Next, cells were washed with PBS and were incubated with 5 μM of **[Ru(DIP)$_2$(gen)](PF$_6$)** or **Ru(DIP)$_2$Cl$_2$** for 2 h (low temperature samples were still kept at 4 ºC). Dilutions were prepared as described in the section "Cytotoxicity assay using a 2D cellular model". Subsequently, cells were washed with PBS, collected, counted and snap frozen in liquid nitrogen. Pellets were stored at -20 ºC. ICP-MS samples were prepared as follows: samples were digested using 70% nitric acid (1 mL, 60 ºC, overnight), further diluted 1:100 (1% HCl solution in MQ water) and analysed using ICP-MS.

Sample Preparation for time-dependent cellular accumulation

MDA-MB-435S and MCF-7 cells were seeded at a density of 3×10^6 in 10 cm plates. The next day, cells were treated with 1 μM concentration of **[Ru(DIP)$_2$(gen)](PF$_6$)**, **Ru(DIP)$_2$Cl$_2$** or cisplatin. Dilutions were prepared as described in the section "Cytotoxicity assay using a 2D cellular model". After 2 h, 12 h, 24 h and 48 h, respectively, the cells were washed, collected, counted and snap frozen in liquid nitrogen and stored until further use at -20 ºC. ICP-MS samples were prepared as follows: samples were digested using 70% nitric acid (0.5 ml for the 2 h and 12 h samples; 1 mL for the 24 h and 48 h samples, 65 ºC, overnight). The samples were further diluted 1:50 (2 h samples) or 1:100 (12 h, 24 h, 48 h samples) in 1% HCl solution in MQ water and analysed using ICP-MS.

ICP-MS studies

All ICP-MS measurements were performed on a high resolution ICP-MS (Element II, ThermoScientific) located at the Institut de physique du globe de Paris (France). The monitored isotopes are ^{101}Ru and ^{195}Pt. Daily, prior to the analytical sequence, the instrument was first tuned to produce maximum sensitivity and stability while also maintaining low uranium oxide formation (UO/U ≤ 5%). The data were treated as follows: intensities were converted into concentrations using uFREASI (user-FRiendly Elemental dAta proceSsIng).[70] This software, developed for HR-ICP-MS users community, is free and available on http://www.ipgp.fr/~tharaud/uFREASI.

ICP-MS data analysis

Cellular uptake studies: The amount of metal detected in the cell samples was transformed from ppb into μg of metal. Data were subsequently normalised to the number of cells and expressed as ng of metal/ amount of cells.

Mechanism of uptake: The amount of ruthenium detected in cell samples was transformed from ppb into μg of ruthenium and values obtained were normalised to the number of cells used for specific treatment. The value for the ruthenium found in the 37 ºC sample was used as a 100%.

Metabolic Studies

HeLa cells were seeded in Seahorse XFe96 well plates at a density of 10×10^3 cells / well in 80 μL. After 24 h, the medium was replaced with fresh medium and cisplatin (1 μM), genistein (1 μM), **$Ru(DIP)_2Cl_2$** (1 μM) or **$[Ru(DIP)_2(gen)](PF_6)$** (1 μM) were added. Dilutions were prepared as described in the section “Cytotoxicity assay using a 2D cellular model”. After 24 h of incubation,

the regular medium was removed, cells were washed thrice using Seahorse Base Media and incubated in a non-CO_2 incubator at 37 °C for 1 h.

Mito Stress Test: Mitostress assay was run using oligomycin, 1 μM, FCCP 1 μM and mixture of antimycin-A/ rotenone 1 μM each in ports A, B and C respectively using Seahorse XFe96 Extracellular Flux Analyzer.

Glycolysis Stress Test: Glycolytic stress test was run using glucose (10 mM), oligomycin (1 μM) and 2-Deoxyglucose (50 mM) in ports A, B and C respectively using Seahorse XFe96 Extracellular Flux Analyzer.

Supporting Information

The Supporting Information is at DOI: XXXXX.

^{1}H-NMR spectrum of **[Ru(DIP)$_2$(5-OHF)](PF$_6$)** (Figure S1), ^{1}H-NMR spectrum of **[Ru(DIP)$_2$(gen)](PF$_6$)** (Figure S2), ^{1}H-NMR spectrum of **[Ru(DIP)$_2$(chr)](OTf)** (Figure S3), ^{1}H-NMR spectrum of **[Ru(DIP)$_2$(mor)](OTf)** (Figure S4), ^{1}H-NMR spectrum of **[Ru(DIP)$_2$(mor)](OTf)** after 5 days in solution (Figure S5), ^{13}C-NMR spectrum of **[Ru(DIP)$_2$(5-OHF)](PF$_6$)** (Figure S6), ^{13}C-NMR spectrum of **[Ru(DIP)$_2$(gen)](PF$_6$)** (Figure S7), ^{13}C-NMR spectrum of **[Ru(DIP)$_2$(chr)](OTf)** (Figure S8), ^{13}C-NMR spectrum of **[Ru(DIP)$_2$(mor)](OTf)** (Figure S9), Overlap of ^{1}H-NMR spectra of **[Ru(DIP)$_2$(5-OHF)](PF$_6$)** in DMSO (Figure S10), Overlap of ^{1}H-NMR spectra of **[Ru(DIP)$_2$(gen)](PF$_6$)** in DMSO (Figure S11), Overlap of ^{1}H-NMR spectra of **[Ru(DIP)$_2$(chr)](OTf)** in DMSO (Figure S12) Overlap of ^{1}H-NMR spectra of **[Ru(DIP)$_2$(mor)](OTf)** in DMF (Figure S13), Fluorometric cell viability assay (Figure S14), Oxygen consumption rates and different respiration parameters in MDA-MB-435S cells alone or after treatment with various test compounds (Figure S15), Extracellular acidification rate and

different parameters during glycolysis in MDA-MB-435S cells alone or after treatment with various test compounds (Figure S16).

Acknowledgements

This work was financially supported by an ERC Consolidator Grant PhotoMedMet to G.G. (GA 681679) and has received support under the program *Investissements d'Aveni*r launched by the French Government and implemented by the ANR with the reference ANR-10-IDEX-0001-02 PSL (G.G.). Ile de France Region is gratefully acknowledged for financial support of 500 MHz NMR spectrometer of Chimie ParisTech in the framework of the SESAME equipment project. We acknowledge the loan of Agilent's equipment to Chimie ParisTech. Part of this work was supported by IPGP multidisciplinary program PARI and by Region Île-de-France SESAME Grant no. 12015908. This project was also financially supported by "Carol Davila" University of Medicine and Pharmacy through Contract no. 23PFE/17.10.2018 funded by the Ministry of Research and Innovation within PNCDI III, Program 1 – Development of the National RD system, Subprogram 1.2 – Institutional Performance – RDI excellence funding projects.

References

(1) Organization, W. H. Noncommunicable diseases https://www.who.int/news-room/fact-sheets/detail/noncommunicable-diseases (accessed Sep 2, 2019).

(2) Hartinger, C. G.; Zorbas-Seifried, S.; Jakupec, M. A.; Kynast, B.; Zorbas, H.; Keppler, B. K. From Bench to Bedside – Preclinical and Early Clinical Development of the Anticancer Agent Indazolium Trans-[Tetrachlorobis(1H-Indazole)Ruthenate(III)] (KP1019 or FFC14A). *J. Inorg. Biochem.* **2006**, *100* (5), 891–904. https://doi.org/https://doi.org/10.1016/j.jinorgbio.2006.02.013.

(3) Oun, R.; Moussa, Y. E.; Wheate, N. J. The Side Effects of Platinum-Based Chemotherapy Drugs: A Review for Chemists. *Dalton Trans.* **2018**, *47* (19), 6645–6653. https://doi.org/10.1039/c8dt00838h.

(4) Boros, E.; Dyson, P. J.; Gasser, G. Classification of Metal-Based Drugs According to Their Mechanisms of Action. *Chem* **2020**, *6* (1), 41–60. https://doi.org/https://doi.org/10.1016/j.chempr.2019.10.013.

(5) Mari, C.; Pierroz, V.; Ferrari, S.; Gasser, G. Combination of Ru(II) Complexes and Light: New Frontiers in Cancer Therapy. *Chem. Sci.* **2015**, *6* (5), 2660–2686. https://doi.org/10.1039/C4SC03759F.

(6) Smith, G. S.; Therrien, B. Targeted and Multifunctional Arene Ruthenium Chemotherapeutics. *Dalt. Trans.* **2011**, *40* (41), 10793–10800. https://doi.org/10.1039/C1DT11007A.

(7) Nazarov, A. A.; Hartinger, C. G.; Dyson, P. J. Opening the Lid on Piano-Stool Complexes: An Account of Ruthenium(II)–Arene Complexes with Medicinal Applications. *J. Organomet. Chem.* **2014**, *751*, 251–260.

https://doi.org/https://doi.org/10.1016/j.jorganchem.2013.09.016.

(8) Zeng, L.; Gupta, P.; Chen, Y.; Wang, E.; Ji, L.; Chao, H.; Chen, Z.-S. The Development of Anticancer Ruthenium(II) Complexes: From Single Molecule Compounds to Nanomaterials. *Chem. Soc. Rev.* **2017**, *46* (19), 5771–5804. https://doi.org/10.1039/C7CS00195A.

(9) Rademaker-Lakhai, J. M.; van den Bongard, D.; Pluim, D.; Beijnen, J. H.; Schellens, J. H. M. A Phase I and Pharmacological Study with Imidazolium-Trans-DMSO-Imidazole-Tetrachlororuthenate, a Novel Ruthenium Anticancer Agent. *Clin. Cancer Res.* **2004**, *10* (11), 3717–3727. https://doi.org/10.1158/1078-0432.CCR-03-0746.

(10) Leijen, S.; Burgers, S. A.; Baas, P.; Pluim, D.; Tibben, M.; Van Werkhoven, E.; Alessio, E.; Sava, G.; Beijnen, J. H.; Schellens, J. H. M. Phase I/II Study with Ruthenium Compound NAMI-A and Gemcitabine in Patients with Non-Small Cell Lung Cancer after First Line Therapy. *Invest. New Drugs* **2015**, *33* (1), 201–214. https://doi.org/10.1007/s10637-014-0179-1.

(11) Hartinger, C. G.; Jakupec, M. A.; Zorbas-Seifried, S.; Groessl, M.; Egger, A.; Berger, W.; Zorbas, H.; Dyson, P. J.; Keppler, B. K. KP1019, A New Redox-Active Anticancer Agent – Preclinical Development and Results of a Clinical Phase I Study in Tumor Patients. *Chem. Biodivers.* **2008**, *5* (10), 2140–2155. https://doi.org/10.1002/cbdv.200890195.

(12) Lentz, F.; Drescher, A.; Lindauer, A.; Henke, M.; Hilger, R. A.; Hartinger, C. G.; Scheulen, M. E.; Dittrich, C.; Keppler, B. K.; Jaehde, U. Pharmacokinetics of a Novel Anticancer Ruthenium Complex (KP1019, FFC14A) in a Phase I Dose-Escalation Study. *Anticancer. Drugs* **2009**, *20* (2), 97–103. https://doi.org/10.1097/CAD.0b013e328322fbc5.

(13) Trondl, R.; Heffeter, P.; Kowol, C. R.; Jakupec, M. A.; Berger, W.; Keppler, B. K. NKP-

1339, the First Ruthenium-Based Anticancer Drug on the Edge to Clinical Application. *Chem. Sci.* **2014**, *5* (8), 2925–2932. https://doi.org/10.1039/C3SC53243G.

(14) Levina, A.; Mitra, A.; Lay, P. A. Recent Developments in Ruthenium Anticancer Drugs. *Metallomics* **2009**, *1* (6), 458–470. https://doi.org/10.1039/b904071d.

(15) Sava, G.; Bergamo, A.; Dyson, P. J. Metal-Based Antitumour Drugs in the Post-Genomic Era: What Comes Next? *Dalt. Trans.* **2011**, *40* (36), 9069–9075. https://doi.org/10.1039/C1DT10522A.

(16) Bergamo, A.; Gaiddon, C.; Schellens, J. H. M.; Beijnen, J. H.; Sava, G. Approaching Tumour Therapy beyond Platinum Drugs: Status of the Art and Perspectives of Ruthenium Drug Candidates. *J. Inorg. Biochem.* **2012**, *106* (1), 90–99. https://doi.org/10.1016/j.jinorgbio.2011.09.030.

(17) Alessio, E. Thirty Years of the Drug Candidate NAMI-A and the Myths in the Field of Ruthenium Anticancer Compounds: A Personal Perspective. *Eur. J. Inorg. Chem.* **2017**, *2017* (12), 1549–1560. https://doi.org/10.1002/ejic.201600986.

(18) Mital, M.; Ziora, Z. Biological Applications of Ru(II) Polypyridyl Complexes. *Coord. Chem. Rev.* **2018**, *375*, 434–458. https://doi.org/https://doi.org/10.1016/j.ccr.2018.02.013.

(19) Notaro, A.; Gasser, G. Monomeric and Dimeric Coordinatively Saturated and Substitutionally Inert Ru(II) Polypyridyl Complexes as Anticancer Drug Candidates. *Chem. Soc. Rev.* **2017**, *46* (23), 7317–7337. https://doi.org/10.1039/C7CS00356K.

(20) Lin, K.; Zhao, Z.-Z.; Bo, H.-B.; Hao, X.-J.; Wang, J.-Q. Applications of Ruthenium Complex in Tumor Diagnosis and Therapy. *Front. Pharmacol.* **2018**, *9*, 1323. https://doi.org/10.3389/fphar.2018.01323.

(21) Salassa, L. Polypyridyl Metal Complexes with Biological Activity. *Eur. J. Inorg. Chem.*

2011, *2011* (32), 4931–4947. https://doi.org/10.1002/ejic.201100376.

(22) Heinemann, F.; Karges, J.; Gasser, G. Critical Overview of the Use of Ru(II) Polypyridyl Complexes as Photosensitizers in One-Photon and Two-Photon Photodynamic Therapy. *Acc. Chem. Res.* **2017**, *50* (11), 2727–2736. https://doi.org/10.1021/acs.accounts.7b00180.

(23) Jakubaszek, M.; Goud, B.; Ferrari, S.; Gasser, G. Mechanisms of Action of Ru(II) Polypyridyl Complexes in Living Cells upon Light Irradiation. *Chem. Commun.* **2018**, *54* (93), 13040–13059. https://doi.org/10.1039/C8CC05928D.

(24) Monro, S.; Colón, K. L.; Yin, H.; Roque, J.; Konda, P.; Gujar, S.; Thummel, R. P.; Lilge, L.; Cameron, C. G.; McFarland, S. A. Transition Metal Complexes and Photodynamic Therapy from a Tumor-Centered Approach: Challenges, Opportunities, and Highlights from the Development of TLD1433. *Chem. Rev.* **2019**, *119* (2), 797–828. https://doi.org/10.1021/acs.chemrev.8b00211.

(25) Intravesical Photodynamic Therapy (PDT) in BCG Refractory/Intolerant Non-Muscle Invasive Bladder Cancer (NMIBC) Patients https://clinicaltrials.gov/ct2/show/NCT03945162 (accessed Sep 5, 2019).

(26) McFarland, S. A.; Mandel, A.; Dumoulin-White, R.; Gasser, G. Metal-Based Photosensitizers for Photodynamic Therapy: The Future of Multimodal Oncology? *Curr. Opin. Chem. Biol.* **2020**, *56*, 23–27. https://doi.org/10.1016/j.cbpa.2019.10.004.

(27) Pettinari, R.; Marchetti, F.; Condello, F.; Pettinari, C.; Lupidi, G.; Scopelliti, R.; Mukhopadhyay, S.; Riedel, T.; Dyson, P. J. Ruthenium(II)–Arene RAPTA Type Complexes Containing Curcumin and Bisdemethoxycurcumin Display Potent and Selective Anticancer Activity. *Organometallics* **2014**, *33* (14), 3709–3715. https://doi.org/10.1021/om500317b.

(28) Kurzwernhart, A.; Kandioller, W.; Bachler, S.; Bartel, C.; Martic, S.; Buczkowska, M.; Muhlgassner, G.; Jakupec, M. A.; Kraatz, H.-B.; Bednarski, P. J.; Arion, V. B.; Marko, D.; Keppler, B. K.; Hartinger, C. G. Structure-Activity Relationships of Targeted $Ru^{II}(\eta^6$-*p*-Cymene) Anticancer Complexes with Flavonol-Derived Ligands. *J. Med. Chem.* **2012**, *55* (23), 10512–10522. https://doi.org/10.1021/jm301376a.

(29) Uivarosi, V.; Munteanu, A.-C.; Nițulescu, G. M. Chapter 2 - An Overview of Synthetic and Semisynthetic Flavonoid Derivatives and Analogues: Perspectives in Drug Discovery; Atta-ur-Rahman, B. T.-S. in N. P. C., Ed.; Elsevier, 2019; Vol. 60, pp 29–84. https://doi.org/https://doi.org/10.1016/B978-0-444-64181-6.00002-4.

(30) Senderowicz, A. M. Flavopiridol: The First Cyclin-Dependent Kinase Inhibitor in Human Clinical Trials. *Invest. New Drugs* **1999**, *17* (3), 313–320.

(31) Jain, S. K.; Bharate, S. B.; Vishwakarma, R. A. Cyclin-Dependent Kinase Inhibition by Flavoalkaloids. *Mini Rev. Med. Chem.* **2012**, *12* (7), 632–649.

(32) Chahar, M. K.; Sharma, N.; Dobhal, M. P.; Joshi, Y. C. Flavonoids: A Versatile Source of Anticancer Drugs. *Pharmacognosy Reviews*. India 2011, pp 1–12. https://doi.org/10.4103/0973-7847.79093.

(33) Singh, M.; Kaur, M.; Silakari, O. Flavones: An Important Scaffold for Medicinal Chemistry. *Eur. J. Med. Chem.* **2014**, *84*, 206–239. https://doi.org/https://doi.org/10.1016/j.ejmech.2014.07.013.

(34) Kumar, S.; Pandey, A. K. Chemistry and Biological Activities of Flavonoids: An Overview. *Sci. J.* **2013**, *2013*, 1–20. https://doi.org/10.1070/RC2004v073n07ABEH000856.

(35) Hostetler, G. L.; Ralston, R. A.; Schwartz, S. J. Flavones: Food Sources, Bioavailability, Metabolism, and Bioactivity. *Adv. Nutr.* **2017**, *8* (3), 423–435.

https://doi.org/10.3945/an.116.012948.

(36) Brastos, I.; Alessio, E.; Ringenberg, M. E.; Rauchfuss, T. B. Ruthenium Complexes. *Inorg. Synth.* **2010**, *35* (Ii), 148–163. https://doi.org/10.1002/9780470651568.ch8.

(37) Caspar, R.; Cordier, C.; Waern, J. B.; Guyard-Duhayon, C.; Gruselle, M.; Le Floch, P.; Amouri, H. A New Family of Mono- and Dicarboxylic Ruthenium Complexes [Ru(DIP) 2 (L 2)] 2+ (DIP = 4,7-Diphenyl-1,10-Phenanthroline): Synthesis, Solution Behavior, and X-Ray Molecular Structure of Trans -[Ru(DIP) 2 (MeOH) 2][OTf] 2. *Inorg. Chem.* **2006**, *45* (10), 4071–4078. https://doi.org/10.1021/ic0601236.

(38) Porter, L. J.; Markham, K. R. The Aluminium(III) Complexes of Hydroxyflavones in Absolute Methanol. Part II. Ligands Containing More than One Chelating Site. *J. Chem. Soc. C Org.* **1970**, *1970*, 1309–1313. https://doi.org/10.1039/J39700001309.

(39) Panhwar, Q. K.; Memon, S. Synthesis and Properties of Zirconium (IV) and Molybdate (II) Morin Complexes. *J. Coord. Chem.* **2012**, No. 65, 37–41.

(40) Naso, L. G.; Lezama, L.; Rojo, T.; Etcheverry, S. B.; Valcarcel, M.; Roura, M.; Salado, C.; Ferrer, E. G.; Williams, P. A. M. Biological Evaluation of Morin and Its New Oxovanadium(IV) Complex as Antio-Xidant and Specific Anti-Cancer Agents. *Chem. Biol. Interact.* **2013**, *206* (2), 289–301. https://doi.org/10.1016/j.cbi.2013.10.006.

(41) Zahirović, A.; Kahrović, E.; Cindrić, M.; Kraljević Pavelić, S.; Hukić, M.; Harej, A.; Turkušić, E. Heteroleptic Ruthenium Bioflavonoid Complexes: From Synthesis to in Vitro Biological Activity. *J. Coord. Chem.* **2017**, *70* (24), 4030–4053. https://doi.org/10.1080/00958972.2017.1409893.

(42) Qi, C.; Xiong, Y.; Eschenbrenner-Lux, V.; Cong, H.; Porco, J. A. Asymmetric Syntheses of the Flavonoid Diels–Alder Natural Products Sanggenons C and O. *J. Am. Chem. Soc.*

2016, *138* (3), 798–801. https://doi.org/10.1021/jacs.5b12778.

(43) Huang, H.; Humbert, N.; Bizet, V.; Patra, M.; Chao, H.; Mazet, C.; Gasser, G. Influence of the Dissolution Solvent on the Cytotoxicity of Octahedral Cationic Ir(III) Hydride Complexes. *J. Organomet. Chem.* **2017**, *839*, 15–18. https://doi.org/https://doi.org/10.1016/j.jorganchem.2016.12.010.

(44) Patra, M.; Joshi, T.; Pierroz, V.; Ingram, K.; Kaiser, M.; Ferrari, S.; Spingler, B.; Keiser, J.; Gasser, G. DMSO-Mediated Ligand Dissociation: Renaissance for Biological Activity of N-Heterocyclic-[Ru(H6-Arene)Cl2] Drug Candidates. *Chem. – A Eur. J.* **2013**, *19* (44), 14768–14772. https://doi.org/10.1002/chem.201303341.

(45) Keller, S.; Ong, Y. C.; Lin, Y.; Cariou, K.; Gasser, G. A Tutorial for the Assessment of the Stability of Organometallic Complexes in Biological Media. *J. Organomet. Chem.* **2019**, 121059. https://doi.org/10.1016/j.jorganchem.2019.121059.

(46) Frei, A.; Rubbiani, R.; Tubafard, S.; Blacque, O.; Anstaett, P.; Felgenträger, A.; Maisch, T.; Spiccia, L.; Gasser, G. Synthesis, Characterization, and Biological Evaluation of New RU(Ii) Polypyridyl Photosensitizers for Photodynamic Therapy. *J. Med. Chem.* **2014**, *57* (17), 7280–7292. https://doi.org/10.1021/jm500566f.

(47) Cepeda, V.; Fuertes, M.; Castilla, J.; Alonso, C.; Quevedo, C.; Perez, J. Biochemical Mechanisms of Cisplatin Cytotoxicity. *Anticancer. Agents Med. Chem.* **2007**, *7* (1), 3–18. https://doi.org/10.2174/187152007779314044.

(48) Keizer, H. G.; Pinedo, H. M.; Schuurhuis, G. J.; Joenje, H. DOXORUBICIN (ADRIAMYCIN): A CRITICAL REVIEW OF FREE RADICAL-DEPENDENT MECHANISMS OF CYTOTOXICITY. *Pharmac. Ther* **1990**, *47*, 219–231. https://doi.org/10.1016/0163-7258(90)90088-J.

(49) Munteanu, A.-C.; Badea, M.; Olar, R.; Silvestro, L.; Mihaila, M.; Brasoveanu, L. I.; Musat, M. G.; Andries, A.; Uivarosi, V. Cytotoxicity Studies, DNA Interaction and Protein Binding of New Al (III), Ga (III) and In (III) Complexes with 5-Hydroxyflavone. *Appl. Organomet. Chem.* **2018**, *32* (12), e4579. https://doi.org/10.1002/aoc.4579.

(50) Deka, B.; Bhattacharyya, A.; Mukherjee, S.; Sarkar, T.; Soni, K.; Banerjee, S.; Saikia, K. K.; Deka, S.; Hussain, A. Ferrocene Conjugated Copper(II) Complexes of Terpyridine and Traditional Chinese Medicine (TCM) Anticancer Ligands Showing Selective Toxicity towards Cancer Cells. *Appl. Organomet. Chem.* **2018**, *32* (4), e4287. https://doi.org/10.1002/aoc.4287.

(51) Roy, S.; Sil, A.; Chakraborty, T. Potentiating Apoptosis and Modulation of P53, Bcl2, and Bax by a Novel Chrysin Ruthenium Complex for Effective Chemotherapeutic Efficacy against Breast Cancer. *J. Cell. Physiol.* **2019**, *234* (4), 4888–4909. https://doi.org/10.1002/jcp.27287.

(52) Spoerlein, C.; Mahal, K.; Schmidt, H.; Schobert, R. Effects of Chrysin, Apigenin, Genistein and Their Homoleptic Copper (II) Complexes on the Growth and Metastatic Potential of Cancer Cells. *J. Inorg. Biochem.* **2013**, *127*, 107–115. https://doi.org/10.1016/j.jinorgbio.2013.07.038.

(53) Fotsis, T.; Pepper, M.; Adlercreutz, H.; Hase, T.; Montesano, R.; Schweigerer, L. Genistein, a Dietary Ingested Isoflavonoid, Inhibits Cell Proliferation and in Vitro Angiogenesis. *J. Nutr.* **1995**, *125* (3 Suppl), 790S-797S. https://doi.org/10.1093/jn/125.suppl_3.790S.

(54) Peterson, G.; Barnes, S. Genistein Stimulated Inhibits Both Proliferation Estrogen and Growth of Human Breast Cancer. *Cell Growth Differ.* **1996**, *7* (October), 1345–1351.

(55) Ullah, M. F.; Ahmad, A.; Zubair, H.; Khan, H. Y.; Wang, Z.; Sarkar, F. H.; Hadi, S. M. Soy

Isoflavone Genistein Induces Cell Death in Breast Cancer Cells through Mobilization of Endogenous Copper Ions and Generation of Reactive Oxygen Species. *Mol. Nutr. Food Res.* **2011**, *55* (4), 553–559. https://doi.org/10.1002/mnfr.201000329.

(56) Marverti, G.; Andrews, P. A. Stimulation of Cis-Diamminedichloroplatinum(II) Accumulation by Modulation of Passive Permeability with Genistein: An Altered Response in Accumulation-Defective Resistant Cells. *Clin. Cancer Res.* **1996**, *2* (6), 991–999.

(57) Spagnuolo, C.; Russo, G. L.; Orhan, I. E.; Habtemariam, S.; Daglia, M.; Sureda, A.; Nabavi, S. F.; Devi, K. P.; Loizzo, M. R.; Tundis, R.; Nabavi, S. M. Genistein and Cancer: Current Status, Challenges, and Future Directions. *Adv. Nutr.* **2015**, *6* (4), 408–419. https://doi.org/10.3945/an.114.008052.

(58) Chambers, A. F. MDA-MB-435 and M14 Cell Lines : Identical but Not M14 Melanoma ? *Perspect. Cancer Res.* **2009**, *63* (13), 5292–5294. https://doi.org/10.1158/0008-5472.CAN-09-1528.

(59) Rae, J. M.; Creighton, C. J.; Meck, J. M.; Haddad, B. R.; Johnson, M. D. MDA-MB-435 Cells Are Derived from M14 Melanoma Cells — a Loss for Breast Cancer , but a Boon for Melanoma Research. *Breast Cancer Res Treat* **2007**, *60*, 13–19. https://doi.org/10.1007/s10549-006-9392-8.

(60) Clède, S.; Lambert, F.; Saint-fort, R.; Plamont, M.; Bertrand, H.; Vessières, A.; Policar, C. Influence of the Side-Chain Length on the Cellular Uptake and the Cytotoxicity of Rhenium Triscarbonyl Derivatives : A Bimodal Infrared and Luminescence Quantitative Study. *Chem. - A Eur. J.* **2014**, *3*, 8714–8722. https://doi.org/10.1002/chem.201402471.

(61) Puckett, C. A.; Barton, J. K. Methods to Explore Cellular Uptake of Ruthenium Complexes. *J. Am. Chem. Soc.* **2007**, *129* (1), 46–47. https://doi.org/10.1021/ja0677564.

(62) Puckett, C. A.; Barton, J. K. Mechanism of Cellular Uptake of a Ruthenium Polypyridyl Complex. *Biochemistry* **2008**, *47* (45), 11711–11716. https://doi.org/10.1021/bi800856t.

(63) Gill, M. R.; Cecchin, D.; Walker, M. G.; Mulla, R. S.; Battaglia, G.; Smythe, C.; Thomas, J. A. Targeting the Endoplasmic Reticulum with a Membrane-Interactive Luminescent Ruthenium(II) Polypyridyl Complex. *Chem. Sci.* **2013**, *4* (12), 4512–4519. https://doi.org/10.1039/c3sc51725j.

(64) Shchepina, L. A.; Pletjushkina, O. Y.; Avetisyan, A. V; Bakeeva, L. E.; Fetisova, E. K.; Izyumov, D. S.; Saprunova, V. B.; Vyssokikh, M. Y.; Chernyak, B. V; Skulachev, V. P. Oligomycin , Inhibitor of the F 0 Part of H + -ATP-Synthase , Suppresses the TNF-Induced Apoptosis. *Oncogene* **2002**, *21*, 8149–8157. https://doi.org/10.1038/sj.onc.1206053.

(65) Inho, K. P.; Youngmi, J.; Pak, K.; Hyewhon, S. B.; Suh, R. S.; Jin, S.; Mei, P.; Zhu, H.; So, I.; Kim, K. W. FCCP Depolarizes Plasma Membrane Potential by Activating Proton and Na + Currents in Bovine Aortic Endothelial Cells. **2002**, 344–352. https://doi.org/10.1007/s004240100703.

(66) Notaro, A.; Frei, A.; Rubbiani, R.; Jakubaszek, M.; Basu, U.; Koch, S.; Mari, C.; Dotou, M.; Blacque, O.; Gouyon, J.; Bedioui, F.; Rotthowe, N.; Winter, R. F.; Goud, B.; Ferrari, S.; Tharaud, M.; Řezáčová, M.; Humajová, J.; Tomšík, P.; Gasser, G. A Ruthenium(II) Complex Containing a Redox-Active Semiquinonate Ligand as Potential Chemotherapeutic Agent: From Synthesis to In Vivo Studies. *ChemRxiv* **2019**. https://doi.org/10.26434/chemrxiv.9582527.v1.

(67) Notaro, A.; Jakubaszek, M.; Rotthowe, N.; Maschietto, F.; Felder, P. S.; Goud, B.; Tharaud, M.; Ciofini, I.; Bedioui, F.; Winter, R. F.; Gasser, G. Increasing the Cytotoxicity of Ru(II) Polypyridyl Complexes by Tuning the Electronic Structure of Dioxo Ligands. *ChemRxiv.*

Prepr. **2019**. https://doi.org/10.26434/chemrxiv.10280507.

(68) Notaro, A.; Jakubaszek, M.; Koch, S.; Rubbiani, R.; Domotor, O.; Enyedy, É. A.; Dotou, M.; Bedioui, F.; Tharaud, M.; Goud, B.; Ferrari, S.; Alessio, E.; Gasser, G. A Maltol-Containing Ruthenium Polypyridyl Complex as a Potential Anticancer Agent. *ChemRxiv. Prepr.* **2019**. https://doi.org/10.26434/chemrxiv.10008917.v1.

(69) Fulmer, G. R.; Miller, A. J. M.; Sherden, N. H.; Gottlieb, H. E.; Nudelman, A.; Stoltz, B. M.; Bercaw, J. E.; Goldberg, K. I. NMR Chemical Shifts of Trace Impurities: Common Laboratory Solvents, Organics, and Gases in Deuterated Solvents Relevant to the Organometallic Chemist. *Organometallics* **2010**, *29* (9), 2176–2179. https://doi.org/10.1021/om100106e.

(70) Tharaud, M.; Gardoll, S.; Khelifi, O.; Benedetti, M. F.; Sivry, Y. UFREASI: User-FRiendly Elemental DAta ProcesSIng. A Free and Easy-to-Use Tool for Elemental Data Treatment. *Microchem. J.* **2015**, *121*, 32–40. https://doi.org/10.1016/j.microc.2015.01.011.

TOC

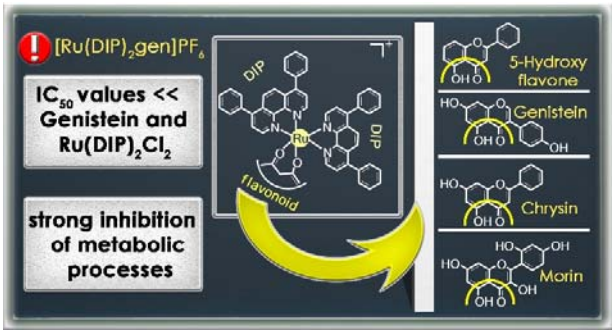

Synopsis

We report the synthesis, characterisation and biological activity of four heteroleptic Ru(II) polypyridyl complexes containing flavonoid ligands. The most promising compound identified in this study was found to strongly inhibit metabolic processes in MDA-MB-435S melanoma cells.

An interesting parallel between this compound and its dichloro precursor highlights the impact of genistein on activity.